

TABLE I
DIELECTRIC PROPERTIES OF $(x)\text{As}_2\text{Te}_3(1-x)\text{As}_2\text{Se}_3$ FOR VARIOUS
COMPOSITIONS AT 300 K

Composition	Dielectric Constant	Loss Tangent
80/20	10.0	0.055
70/30	9.3	0.049
60/40	7.9	0.042
50/50	7.2	0.030
40/60	7.0	0.020

I. No observable variation occurred in either the dielectric constant or loss tangent over the temperature range -193-353 K. The results for the various compositions were exactly the same as those obtained in the earlier study of frequency dependence [6].

One of the samples $(80)\text{As}_2\text{Te}_3(20)\text{As}_2\text{Se}_3$ was tested in the far-infrared region from 5 K to room temperature [7]. The sample exhibited essentially constant transmission properties over the entire temperature range.

IV. CONCLUSIONS

The amorphous system $(x)\text{As}_2\text{Te}_3(1-x)\text{As}_2\text{Se}_3$ exhibits characteristics that appear to make them useful as microwave dielectric materials. The high dielectric constant and low loss tangent which is easily controlled by compositional variation, remains constant from 0.5 to 18 GHz over the temperature range from -80 to +80°C. The material is easily worked to a smooth finish suitable for high-quality thick films and substrates.

Preliminary tests indicate that the dielectric properties are constant at even higher frequencies and lower temperatures but some variation was noted above 80°C. Since the materials have relatively low softening temperatures, their use for applications above 100°C would be somewhat restricted [1].

ACKNOWLEDGMENT

The authors wish to thank K. Button of the Massachusetts Institute of Technology for the measurements in the far-infrared region.

REFERENCES

- [1] D. L. Kinser, L. K. Wilson, H. R. Sanders, and D. J. Hill, *J. Non-Crystalline Solids*, vol. 8, no. 10, p. 823, 1972.
- [2] H. R. Sanders, D. L. Kinser, and L. K. Wilson, in *Proc. 9th Annu. IEEE Region III Conv.*, 1971, p. 429.
- [3] M. N. Roilos, *J. Non-Crystalline Solids*, vol. 6, p. 5, 1971.
- [4] B. T. Kolomietz and T. F. Nazarova, *Sov. Phys.—Solid State*, vol. 2, p. 369, 1960.
- [5] A. R. Von Hippel, *Dielectric Materials and Applications*, New York: M.I.T. Technology Press, 1954.
- [6] J. D. Pearson, G. T. O'Reilly, and L. K. Wilson, in *Proc. 10th Annu. IEEE Region III Conv.*, 1971, pp. G6-1-G6-3.
- [7] K. Button, private communication, M.I.T., Cambridge, Mass.

Anomalies in Duplexing Very Short Pulses

D. J. FITZGERALD AND J. M. PROUD

The advent of nanosecond pulse sources with multikilowatt power at X band [1] has created a need for a suitable duplexing scheme for incorporation into a monostatic radar configuration. The advantages and disadvantages of various ferrite and diode duplexer structures have been evaluated. It is the purpose of this letter to report these results and to indicate several phenomena that were observed to be unique to short-pulse operation.

An IKOR Cavatron short-pulse source that generates a damped sinusoidal output waveform, as shown in Fig. 1, was used in the

Manuscript received November 5, 1973. This work was supported in part by the Air Force Avionics Laboratory, Wright-Patterson AFB under Contract F33615-72-C-1930.

The authors are with IKOR, Inc., Burlington, Mass. 01803.

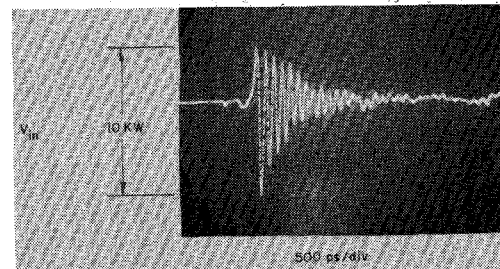


Fig. 1. Short-pulse transmitter—typical RF output.

duplexer evaluations. It has an X-band output power spectrum with a half-power bandwidth of 0.2 GHz, while the peak power is variable up to 20 kW.

A schematic of the three basic duplexer configurations evaluated is shown in Fig. 2. All are active devices utilizing p-i-n diode switching properties or a combination of ferrite circulator and p-i-n diode switching action.

Referring to Fig. 2(a), the two shunt-mounted diodes constitute a simple TEM switching structure with low-level short-pulse transmission properties similar to those observed with a CW signal. However, with the diodes reverse biased under intense short-pulse field conditions, the capacitive reactance of the diodes becomes shunted by a large RF voltage-dependent conductance. As a consequence, the insertion loss of the switch increases with applied power, as shown in Fig. 3. It appears that electrons and holes present in equilibrium in the diode's I region are accelerated, giving rise to bulk ionization of the lattice structure, which develops into a controllable avalanche. The effect is reversible and does not permanently impair the diode's characteristics.

Again referring to Fig. 2(a), the circulator is a waveguide partial-height ferrite Y junction being connected to the diode switch structure via a coaxial-to-waveguide transducer. A very short pulse propagating in a waveguide is subject to dispersion [2], which causes distortion of both the envelope and the carrier wave of the pulse. Thus the short-pulse transmission losses are measured with respect to the transmission through an approximate equivalent length of waveguide. Fig. 4 illustrates the circulator's forward (low-loss) transmission path properties. The insertion loss is 0.4 dB greater than the measured CW value, while the pulse shape is relatively distortionless. Note, if the short-pulse spectrum does not fall within the passband of the circulator, severe pulse elongation will occur. The short-pulse isolation is only 17 dB compared to the greater than 27 dB measured with a CW signal. The exact nature of the isolation degradation is not understood. Others [3] have reported excessive spike leakage with ferrites; however, an explanation of this occurrence will require further investigation.

The balanced duplexer configuration of Fig. 2(b) utilizes two diode switches identical to that previously described in the ferrite/diode duplexer. The hybrids are constructed in stripline using a standard quarter-wavelength overlay technique. The transmission losses of short pulses through this duplexer are comparable to the measured CW data, other than the nonlinearities introduced by the reverse-biased diodes. Further, short-pulse transmission is relatively distortionless, though the hybrids do appear to alter the relative height of the first half-cycle of the pulse. Due to breakdown in the overlay coupling structure, power handling is limited to 18 kW. In general, the short-pulse breakdown voltage is much greater than the CW breakdown since the buildup of ionization, or the formative time, is comparable to pulselength [4].

The modified branched duplexer, Fig. 2(c), is not particularly

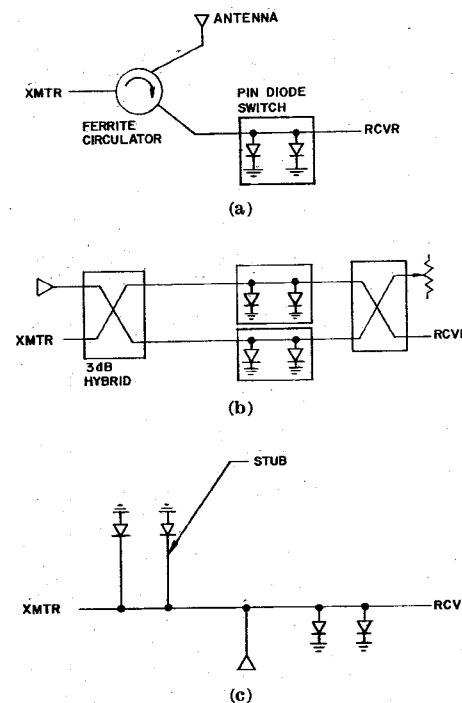


Fig. 2. Basic duplexers. (a) Circulator and semiconductor switch configuration. (b) Balanced semiconductor configuration. (c) Modified branched semiconductor configuration.

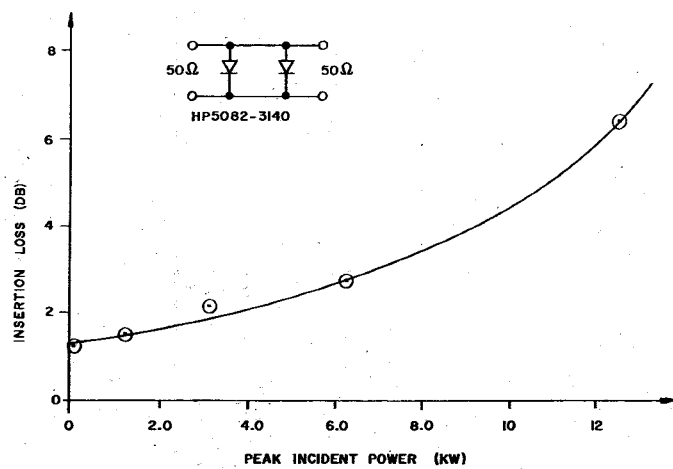


Fig. 3. Short-pulse effect on a reverse-biased diode switch.

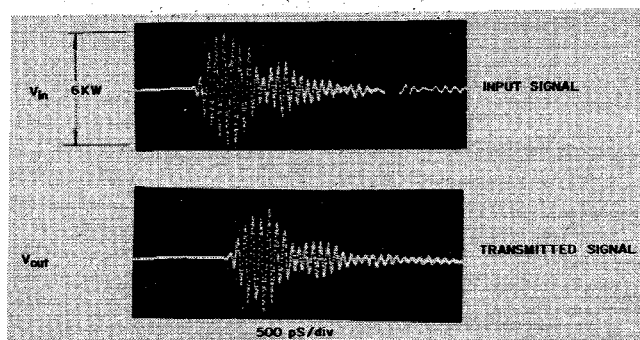


Fig. 4. Circulator's short-pulse forward transmission characteristics.

TABLE I
COMPARISON OF CW AND PULSE DUPLEXER CHARACTERISTICS

Duplexer	Ferrite/Diode		Balanced		Modified Branch	
	CW	Pulse	CW	Pulse	CW	Pulse
Transmit Loss	.4 dB	.8 dB	1.5 dB	1.3 dB	1.2 dB	5.3 dB
Rec. Loss	1.6 dB	2.1 dB ^a	2.1 dB	2.7 dB ^a	1.7 dB	2.5 dB ^a
Power Handling	—	> 20 kW	—	18 kW	—	> 20 kW
Rec. Isolation	> 57 dB	> 57 dB	> 50 dB	> 50 dB	> 50 dB	> 50 dB
Switching (includes driver)	135 ns	135 ns	135 ns	135 ns	135 ns	135 ns
Pulse Fidelity	—	good	—	fair	—	poor

^a For low-level input.

suit to short-pulse operation due to the high transmit loss of 5.3 dB. This is caused by the ineffectiveness of the diode-loaded stubs that are required to introduce a shunt open circuit across the transmitter-to-antenna branch of the structure. The electric field build-up time and the nonuniformity of the pulse amplitude are not conducive to establishing the appropriate field conditions.

A brief summary and comparison of the short-pulse and CW performance of the duplexers are given in Table I. Of the several duplexers investigated, the combination of ferrite circulator and shunt-mounted diode switch is most suited to duplexing of short-pulse signals. It offers high-fidelity transmission with the least attenuation of transmit and receive signals.

REFERENCES

- [1] J. M. Proud *et al.*, "Short pulse radar generators," Air Force Avionics Lab., Wright-Patterson AFB, Tech. Rep. AFAL-TR-72-41, Mar. 1972.
- [2] M. Ito, "Dispersion of very short microwave pulses in waveguide," *IEEE Trans. Microwave Theory Tech.*, vol. MTT-13, pp. 357-364, May 1965.
- [3] K. G. Narayanan and G. P. Sharma, "Isolation rating of ferrite components at high pulse powers," *IEEE Trans. Microwave Theory Tech. (Corresp.)*, vol. MTT-18, pp. 322-323, June 1970.
- [4] P. Felsenfeld and J. M. Proud, "Nanosecond-pulse breakdown in gases," *Phys. Rev.*, vol. 193, pp. A1796-A1804, Sept. 1965.

Addenda to "The Exact Dimensions of a Family of Rectangular Coaxial Lines with Given Impedance"

HENRY J. RIBLET

When the above paper¹ was written, it was the writer's opinion that the Bowman [1] reference was the best available. Quite by chance, while searching the literature in another connection, he encountered a reference made by Anderson [2] to a paper by Bergmann [3] in which the same problem is solved with the same results and methods. Oddly enough Bergmann's paper, considering the general case, predates Bowman's solution of the special case by ten years.

There are a few minor differences which may be noted at this time as follows.

1) Bergmann's restriction [3, eq. (1)¹] that $\lambda < k < 1$, is more restrictive than my comparable condition $0 < \alpha < \beta$ and $\alpha\beta < 1$, since the condition $\beta < 1$ ignores one of two possible orientations of the figure.

¹ Manuscript received November 7, 1973.
The author is with Microwave Development Laboratories, Inc., Needham, Mass.
² H. J. Riblet, *IEEE Trans. Microwave Theory Tech.*, vol. MTT-20, pp. 538-541, Aug. 1972.

2) My evaluation of the multivalued elliptic integrals by plotting the path of integrations on the $R(k)$ and $R(\lambda)$ surfaces appears to represent a substantial simplification of the solution.

3) Bergmann has given necessary and sufficient conditions that a given system of concentric rectangles belong to the family under consideration. Applying arguments similar to Bergmann's to equation (11),¹ we have

$$\frac{\overline{QA} + \overline{CB}}{\overline{AB}} = \frac{K(\lambda)}{K'(\lambda)} \quad \text{and} \quad \frac{\overline{DC} + \overline{EO}}{\overline{DE}} = \frac{K'(k)}{K(k)}. \quad (\text{A})$$

Thus the ratios of the dimensions of any rectangular system uniquely determine λ and k . In addition,

$$\frac{\overline{AB}}{\overline{DE}} = \frac{K'(\lambda)}{K(k)}. \quad (\text{B})$$

Now, if this condition is satisfied after λ and k have been determined from the dimensions of the given system of concentric rectangles, it is not difficult to show that the α and β determined by (3)¹ have the property that $0 < \alpha < \beta$ and $\alpha\beta < 1$, and moreover that the rectangles given by equation (11)¹ differ at most by a scale factor from the given rectangles. Thus condition (B) is sufficient as well as necessary.

Perhaps it is even more useful to observe that the solution given first by Bergmann and then the writer can be extended to map the upper half of the complex plane into the interior of a symmetrical *U*-shaped region. This permits the determination of the characteristic impedance of the same class of concentric rectangular conductors with the difference that one or more walls may be magnetic in an asymmetrical manner.

To see how this is possible, consider the transformation,

$$z = \int_0^u \frac{M(1-u^2)^{1/2} du}{[(a^2-u^2)(b^2-u^2)(c^2-u^2)]^{1/2}} \quad (1)$$

which maps the upper half of the u plane in Fig. 1 into the interior of the *U*-shaped figure in the z plane which is symmetrical about the imaginary axis, for M real and positive. Then the transformation $v = u^2$ maps the upper left-hand quadrant of the u plane into the lower half of the v plane. Consequently, when this substitution is made in (1), it follows that

$$z = \frac{M}{2} \int_0^v \frac{(1-v)^{1/2} dv}{[v(a^2-v)(b^2-v)(c^2-v)]^{1/2}} \quad (2)$$

maps the lower half of the v plane into the *L*-shaped figure in the z plane which is just that half of the *U*-shaped figure which lies in the left-half plane, since values on the negative v axis correspond to imaginary values of z . Here again, corresponding boundary points are denoted by the same capital letters.

Now the further transformation

$$v = \frac{1-w}{1-\alpha\beta w} \quad (3)$$

maps the lower half of the v plane onto the upper half of the w plane whenever $\alpha\beta < 1$. Then, if we select a , b , and c so that

$$a^2 = \frac{1+\alpha}{\alpha(1+\beta)} \quad b^2 = \frac{1+\beta}{\beta(1+\alpha)} \quad c^2 = \frac{1}{\alpha\beta} \quad (4)$$

the substitution of (3) in (2) results in the transformation

$$z = M' \int_1^w \frac{w^{1/2} dw}{[(1-w)(1+\alpha w)(1+\beta w)(1-\alpha\beta w)]^{1/2}} \quad (5)$$

which maps the upper half of the w plane into the same *L*-shaped figure in the z plane. However, the coordinates of the points on the real axis of the w plane corresponding to the corners of the figure in the left half of the z plane are given in terms of α and β . Here $M' = M\alpha\beta(1+\alpha)^{1/2}(1+\beta)^{1/2}/2$ and any ambiguity of sign is resolved by noting that the integral in (5) differs at most by an additive constant from an integral, equation (1), which is known to map the upper half w plane into an *L*-shaped region in the z plane having this orientation.